Evaluation of TA SD's energy reconstruction performance using a DNN and hybrid data

Anton Prosekin[1], Kozo Fujisue[1],
Anatoli Fedynitch[1,2], and Hiroyuki Sagawa[2]
for the Telescope Array Collaboration

[1]Institute of Physics, Academia Sinica,
[2]Institute for Cosmic Ray Research

UHECR 2024, 17-21 November 2024

Motivation: Mass on event-by-event basis

Propagation:

- Magnetic fields deflects UHECR in dependence of rigidity R ~ E/Z (typically Z = 1 - 26)

- Type of the particle determines the maximal distance (horizon) to the potential source

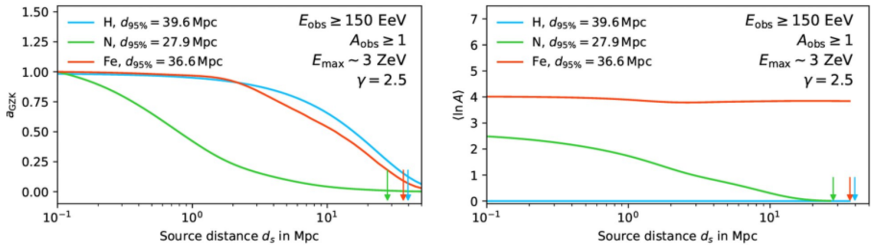

N. Globus, A. Fedynitch, R. Blandford, 2022

Large impact of Galactic magnetic fields:
For example particle E=60 EeV and Z=?:
arrived from **outside galaxy points to**

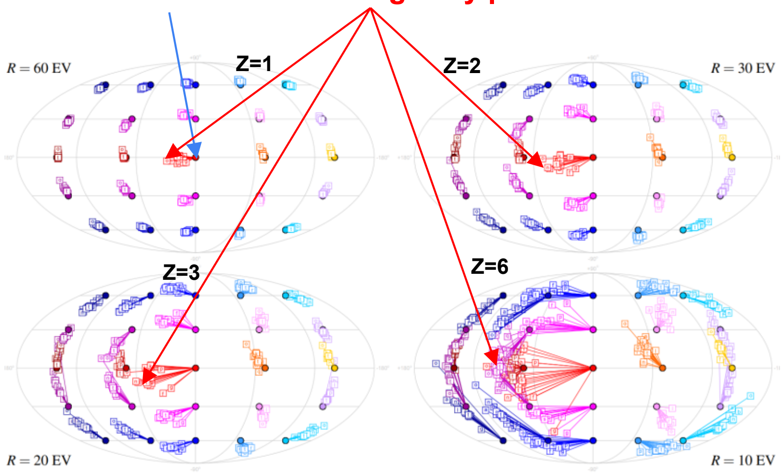

M.Unger, G. Farrar, ICRC2017

Backtracking of particles for different models of the coherent GMF

Source properties:

- Acceleration at the source: maximum rigidity is determined by acceleration
- Mass composition at the source

Mass reconstruction

- Fluorescence Detector (FD):
  - Directly observe X_{max} as an estimator for mass composition
  - Limited statistics with duty cycle 10%

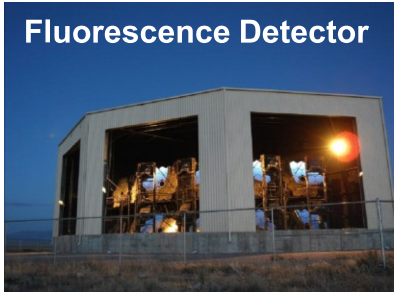

- Surface Detector (SD):
  - Large statistics with duty cycle 100%
  - Can be used to extract primary mass via a number composition-related observables
  - Extraction requires complicated analysis techniques with feature engineering
  - DNN can automatically extract the most relevant features from the raw SD data

DNN approach

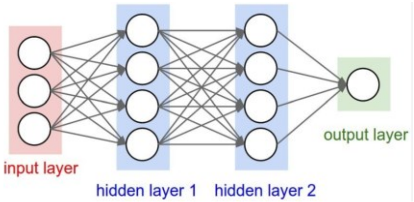

Simple DNN representation

Deep Neural Network (DNN) vs. Standard reconstruction:

- Learns complex non-linear patterns vs. physics-based constructed features
- More robust to various uncertainties and shower-to-shower fluctuations
- Generalize well to new events, allowing for reliable estimation on an event-by-event basis
- Can use all shower data (time traces) vs. integral features (arrival times, total signal)
  - can extract complex features (X_{max}, R_μ, A) $\Leftarrow$ *final objective*
  - **more accurate reconstruction ⇒ boosting statistics with relaxed quality cuts** $\Leftarrow$ *this talk*

Time traces of surface detectors

Standard reconstruction uses:
1. geometry
2. arrival times
3. total signal

Time traces: 1-4 segments of 128-bin time series of 20 ns x 2 channels (upper/lower)

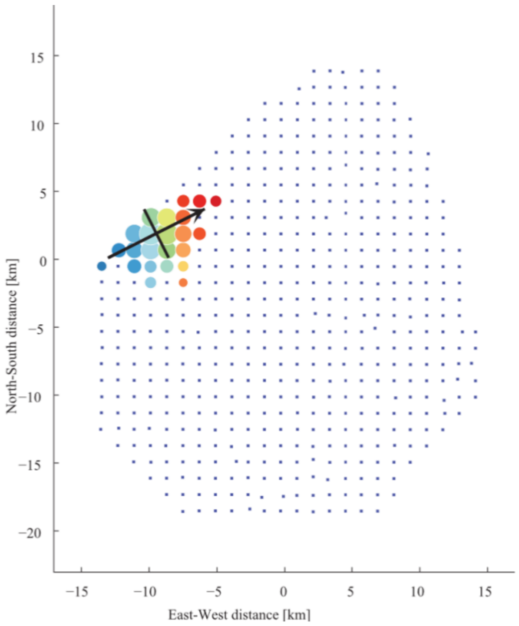

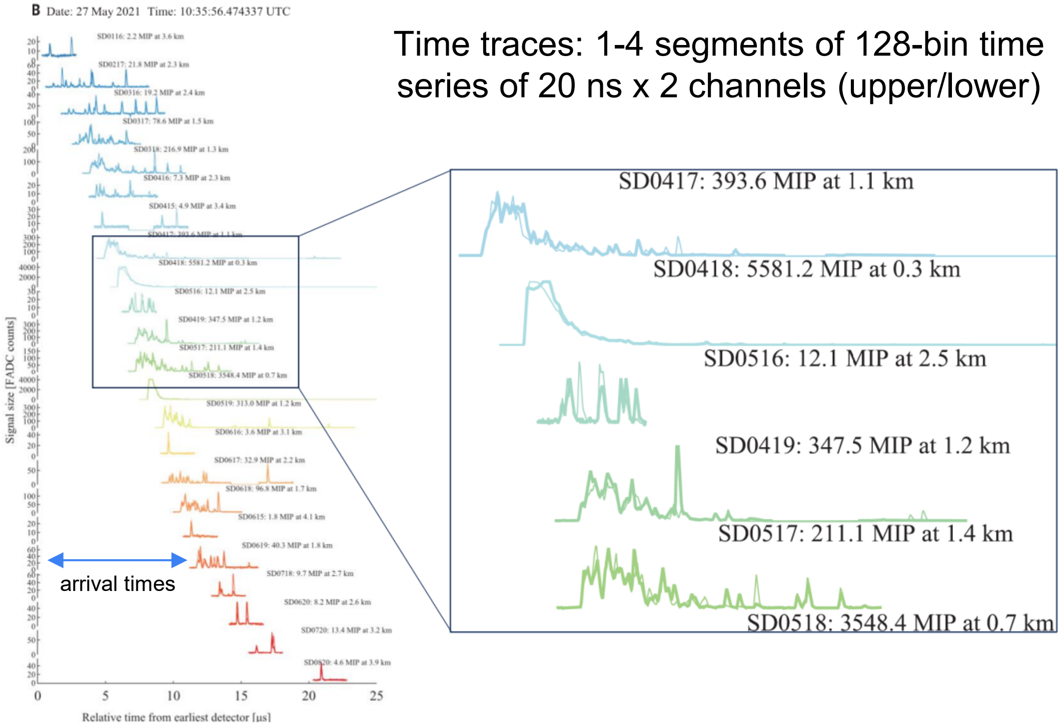

Time traces and surface detector footprint for highest registered event of TA E=244 EeV (Science 382, 903 (2023))

Content of surface detector signals

- Arrival times → front curvature → shower **direction** and **core** position
- Total signal → **energy** of primary particle
- Time trace → front width and structure → development of
  - electromagnetic and muonic component
- Dynamics (time traces shape) of components encodes
  - complex feature
  - additional information for energy, direction, core position

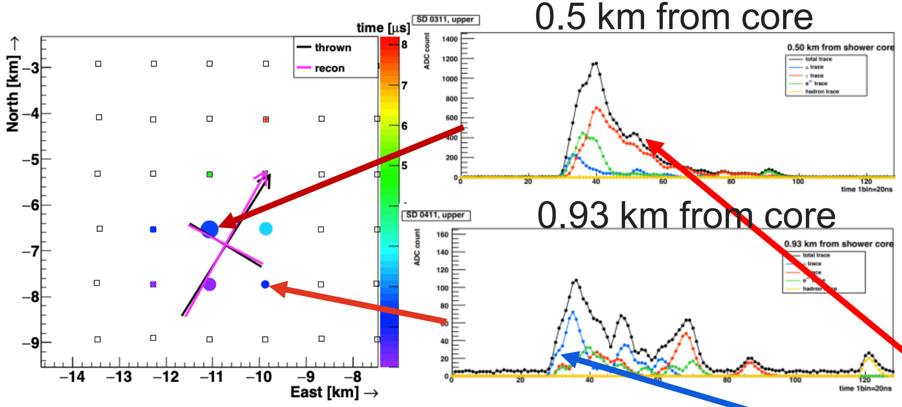

TA MC simulations

K. Fujita, 2024

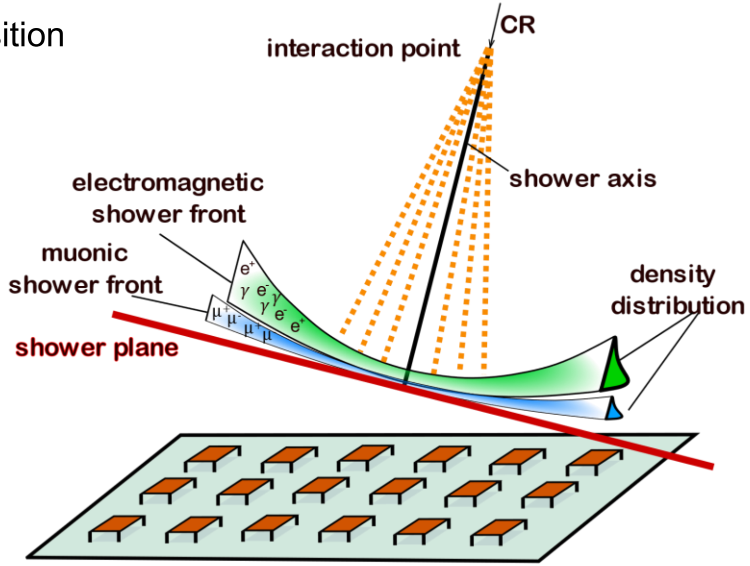

TA SD array

Mass composition information:

- X_{max} information from electromagnetic component
- R_{μ} (number of muons) information from the early part of the time trace (and early shower evolution)

DNN conceptual scheme

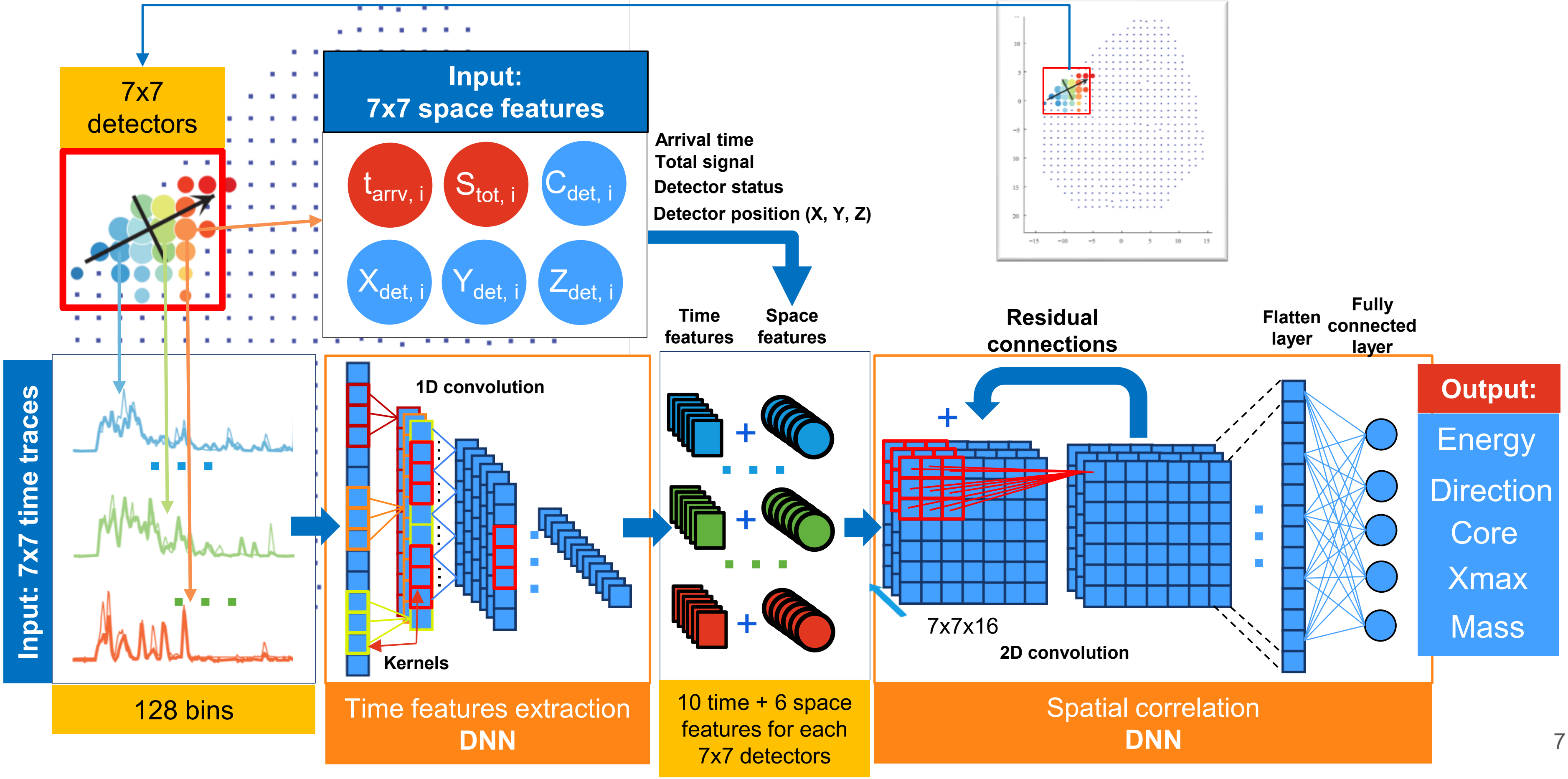

AixNet DNN architecture

AixNet was originally developed by Auger collaboration
(M. Erdmann, J. Glombitza, D. Walz, 2018):

- Time feature extraction DNN consists of 3 layers of 1D CNN
  - Kernel size and stride should be adjusted for each layer
  - Typically: kernel size = 7, and stride = 4
  - Use 2 time traces
- Spatial correlation DNN consist of 7 layers Depthwise Separable Convolution CNN:
  - performs spatial convolutions (2D) separately on each of 7x7 “feature” map
  - correlating all feature maps pixel-wise
  - Skip (residual) connections concatenate output with input of previous layer
- Fully-connected layer (FC) transforms flattened features to predicted quantities:
  - E(1), core axis (3), core position(2), X_{max}(1), mass vector(4)

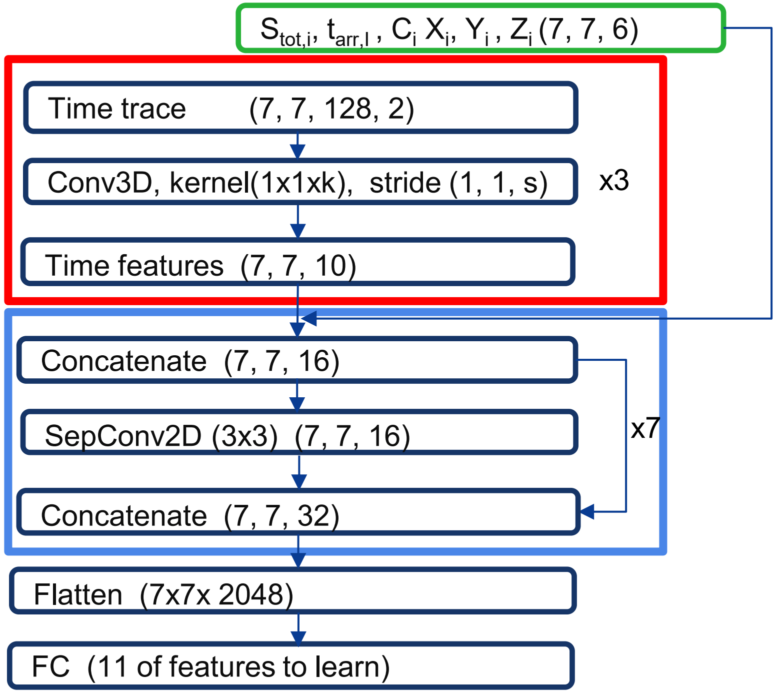

Event’s tiles

- Each event is represented as NxN tile of detectors
- 7x7 vs 9x9 have similar results
    - Use 7x7 to save memory and calculation time
- Tile is centered on detector with **largest integrated** signal
- Mask central detector (by zeros) because of:
    - strongest signal → saturation
    - closest to the core → MC might not correctly model signal
- Some detectors in the tile might be broken or not exist (border case):
    - Missing information reduce accuracy of reconstruction

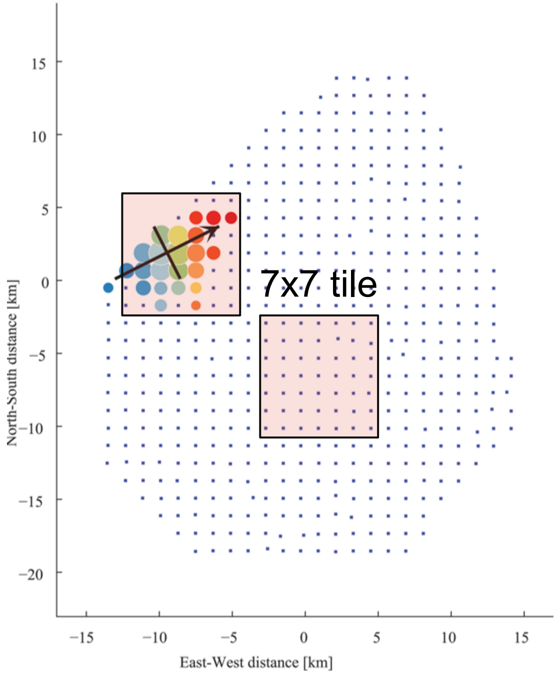

Standard reconstruction

Standard reconstruction is **parameter fitting** of set of <u>phenomenological functions</u> via **χ^2 minimization** on <u>total signal</u> and <u>arrival times</u> data:

1. Geometry estimates:

- Core position
- Shower axis projection

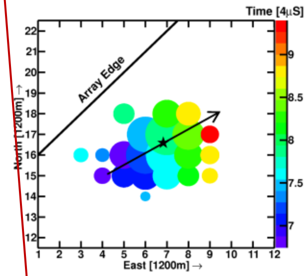

$$(R_{\rm COG})_k = \frac{\sum_{i=1}^{N} \rho_i \, (r_i)_k}{\sum_{i=1}^{N} \rho_i},$$

$$M_{jk} = \frac{\sum_{i=1}^{N} \rho_i \left[(r_i)_j - (R_{\rm COG})_j\right]\left[(r_i)_k - (R_{\rm COG})_k\right]}{\sum_{i=1}^{N} \rho_i}$$

2. Plane wave front estimates:

- Arrival time T_0
- Zenith angle $\sin(\theta)$

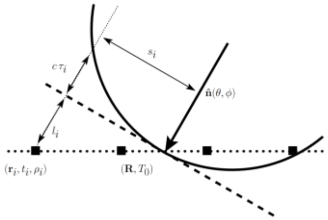

$$t = T_0 + \frac{l}{c} = T_0 + [\sin(\theta)] \, \frac{(\mathbf{r} - \mathbf{R}) \cdot \hat{\mathbf{u}}}{c}$$

3. Time fit minimization:

- Minimization against core, zenith angle, arrival time
- Linsley time delay function

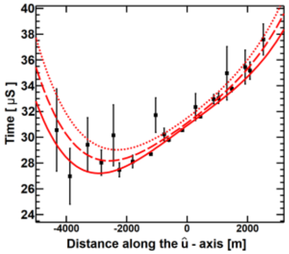

$$\chi^2_{\rm G} = \sum_{i=0}^{N} \frac{(t_i - t_i^{\rm FIT})^2}{\sigma^2_{t_i}} + \frac{(\mathbf{R} - \mathbf{R}_{\rm COG})^2}{\sigma^2_{\mathbf{R}_{\rm COG}}}$$

$$t^{\rm FIT} = T_0 + \frac{l}{c} + \tau$$

$$\tau = (8 \times 10^{-4} \mu{\rm S}) \, a(\theta) \left(1.0 + \frac{s}{30{\rm m}}\right)^{1.5} \rho^{-0.5}$$

4. Lateral distribution fit:

- Minimization against core, LDF scale function
- LDF AGASA function

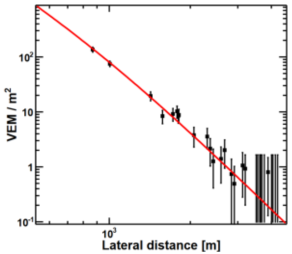

$$\chi^2_{\rm LDF} = \sum_{i=0}^{N} \frac{(\rho_i - \rho_i^{\rm FIT})^2}{\sigma^2_{\rho_i}} + \frac{(\mathbf{R} - \mathbf{R}_{\rm COG})^2}{\sigma^2_{\mathbf{R}_{\rm COG}}}$$

$$\rho = A \left(\frac{s}{91.6{\rm m}}\right)^{-1.2} \left(1 + \frac{s}{91.6{\rm m}}\right)^{-(\eta(\theta)-1.2)} \times \left(1 + \left[\frac{s}{1000{\rm m}}\right]^2\right)^{-0.6}$$

Standard reconstruction

1. First energy estimation:

- Energy evaluated from Energy Estimation Table using reconstructed sec(θ) and S800 = ρ(800 m)
- Energy Estimation Table is build from large statistics MC set with **characteristics of real data** by using standard reconstruction
- MC dataset with **QGSJET-II-03** interaction model and pure proton composition has been used

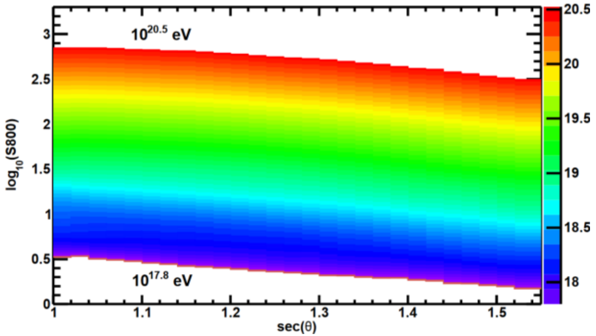

TA SD Energy Estimation Table,
CORSIKA MC simulations with **QGSJET-II-03**
for protons

2. Energy scale calibration

- First energy estimation is scaled using calibration of SD against the FD measurements on hybrid data
- **E_{SD} scaled 1/1.27 to FD Energy**

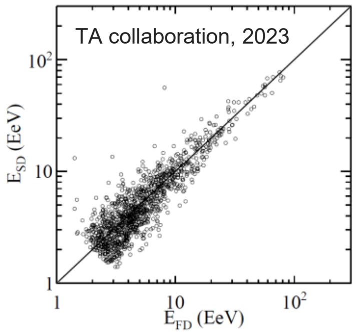

Other reconstruction methods:

- **Constant intensity cuts (CIC) doesn't use MC**
- CIC agrees with results of standard reconstruction (see Jihyun Kim's talk)

MC data set details

- CORSIKA 7.3500 simulations
- QGSJet-II-04
- p, He, N, Fe (0.5 M each)
- 1000 x 26 x 4 x 20 ~ 2 M events
  - 1000 Corsika showers per energy bin
  - 26 energy bins
  - 4 elements
  - 20 reshuffling per shower
- Energies: (1 EeV, 300 EeV), E^-1 distribution, 26 bins
- Zenith angles: < 70 deg, isotropic distribution
- Training/validation: 0.9/0.1
- Test set ~ 0.5 M
- Standard spectral quality cuts

Spectral quality cuts

Cut	Efficiency, %	Combined, %
$N_{SD} \geq 5$	89.82	89.82
$\theta < 45°$	59.08	52.75
$D_{border} \geq 1200$ m	71.28	38.43
χ^2_G/d.o.f. < 4, χ^2_{LDF}/d.o.f. < 4	80.64	34.07
$(\sigma^2_\theta + \sin^2\theta\, \sigma^2_\varphi)^{(1/2)} < 5°$	87.43	31.60
$\sigma_{S800}/S800 < 0.25$	69.35	29.34

SD energy reconstruction

DNN reconstruction

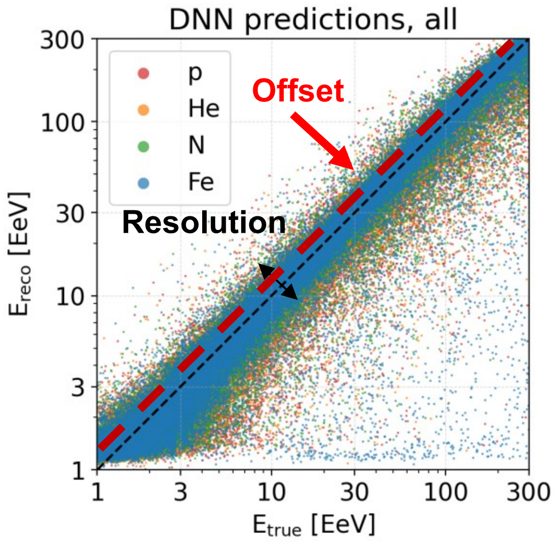

Quality cuts

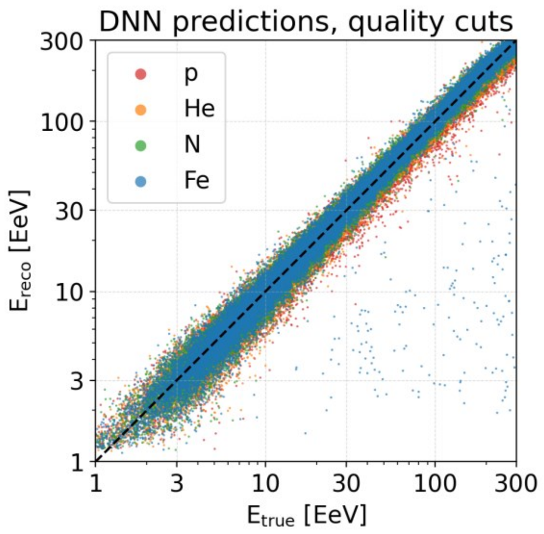

SD energy reconstruction offset

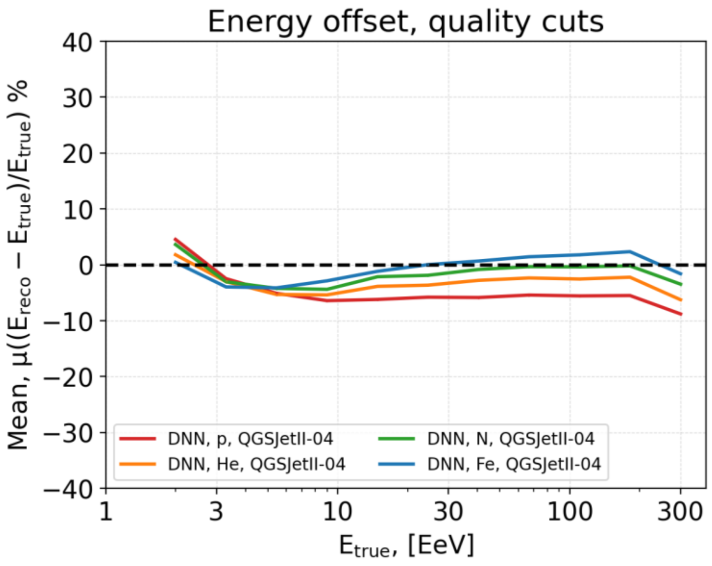

- Reconstruction is applied to:
  - MC simulations with **QGSJet II-04**
  - events passed quality cuts

- DNN trained on **QGSJet II-04**:
  - tends to center around zero bias
  - energy offsets -6% – +2.5% (at 200 EeV)
  - offset depends on mass of primary with spread 8.5 %
  - curves are ordered from proton (red) to iron (blue)

- The reconstruction offset depends on interaction model and primary mass and should be fixed by calibration against hybrid events (intrinsically correct interaction and composition)

Energy offsets for other models

Comparison with QGSJet II-03

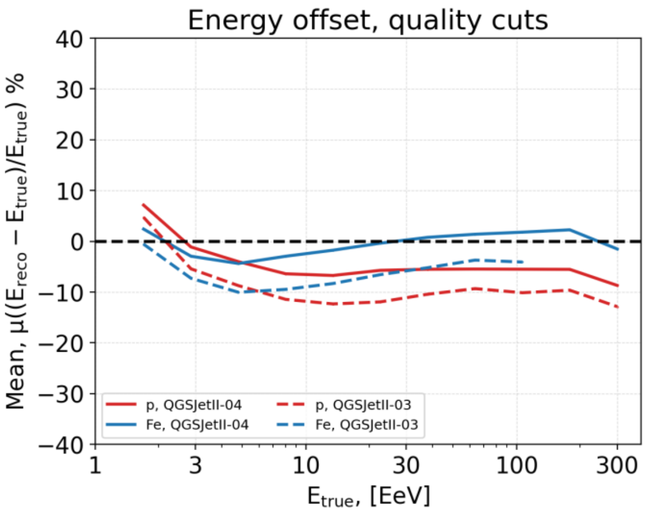

Comparison with Sibyll 2.3d

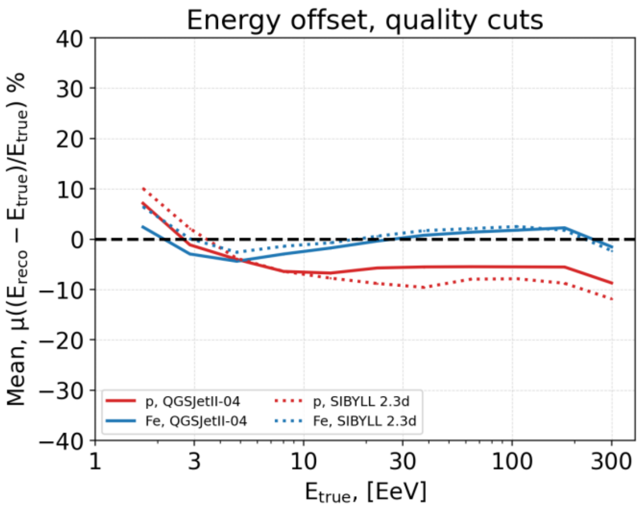

- For interaction models different from training model the offset changed no more than 7%
- Offsets between p and Fe are within 10% and ordered the same way

Energy offsets: DNN vs standard reconstruction

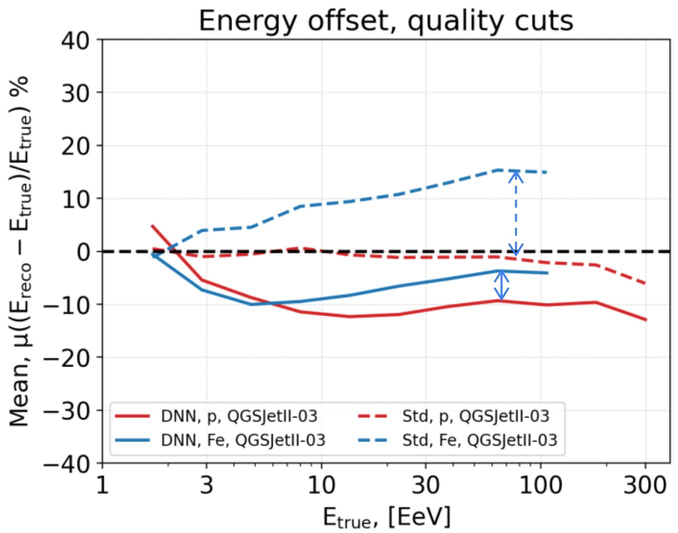

- Standard reconstruction is adjusted to **QGSJetII-03 proton** MC simulations
- Offset difference between p and Fe for DNN reconstruction are smaller than in standard reconstruction:
  - DNN still has composition dependent offset but adapts to it better than standard reconstruction

SD energy resolution

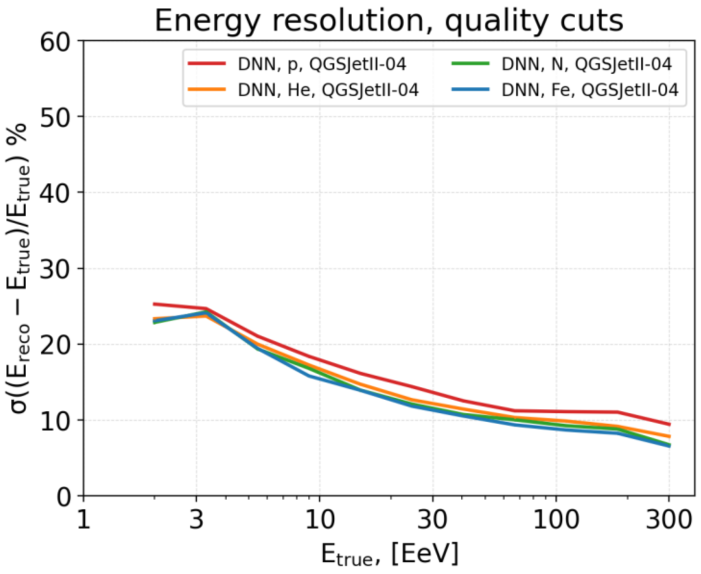

- The same events as for offset (same caveats)
- Resolution (spread) does not depend on offset
- Resolution weakly depends on composition
- DNN energy resolution:
  - protons: 8% - 25%
  - He, N, Fe: slightly better than protons

Energy resolution for other models

Comparison with QGSJetII-03

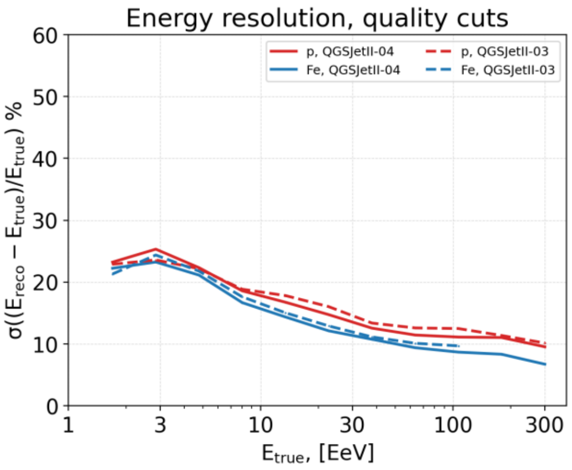

Comparison with Sibyll 2.3d

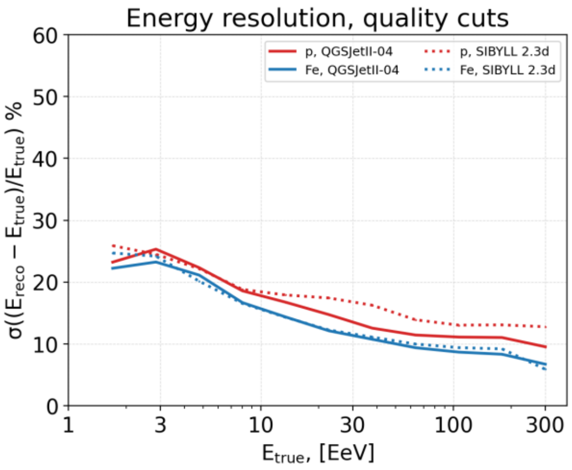

- Resolution is very similar between models with weak dependence on type of primary

SD energy resolution: DNN vs Std

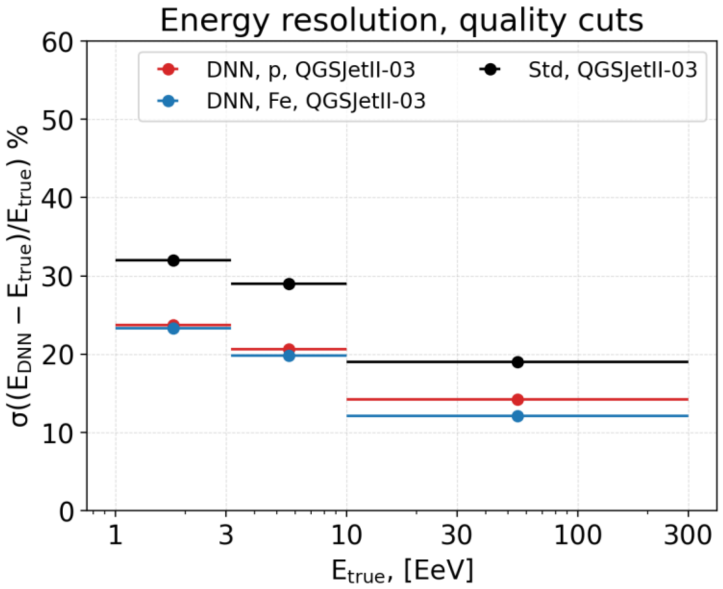

- Resolution is more difficult to take into account than offset, i.e. the smaller the resolution the better
- DNN notably improves resolution compared to standard reconstruction

DNN and quality cuts

DNN reconstruction on events that pass quality cuts and on the events that do not (“other”)

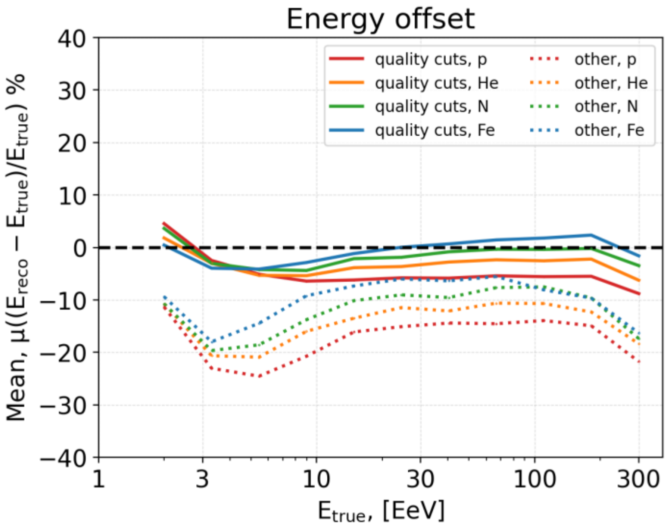

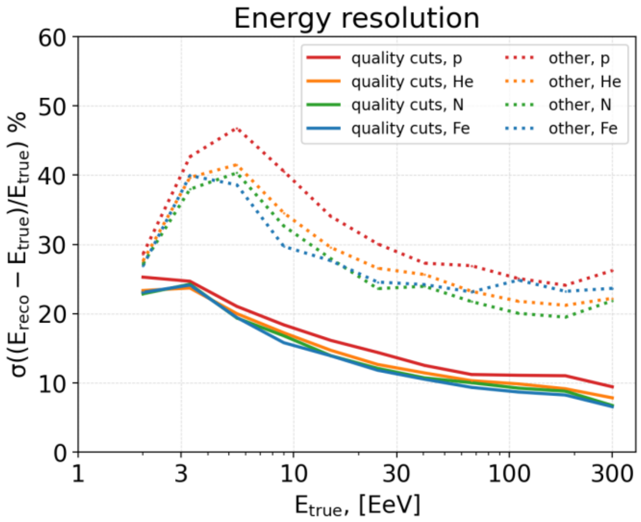

DNN improved resolution will allow

- Search for **more relaxed quality cuts** while maintaining the good resolution of the existing reconstruction - **increasing statistics**

Directional reconstruction

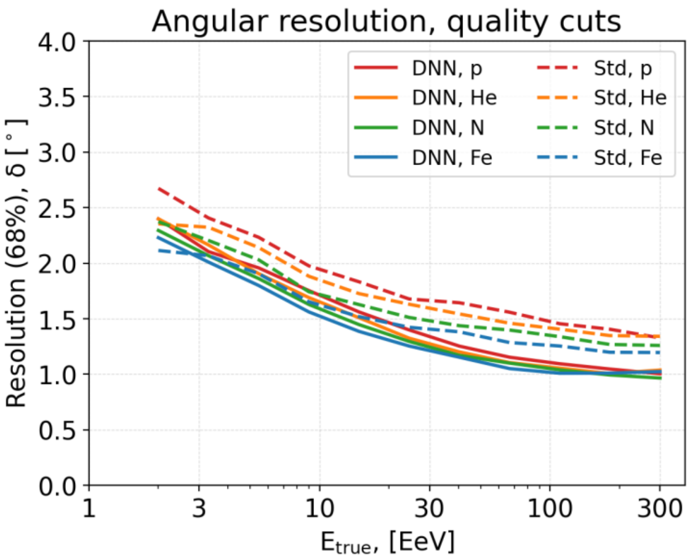

- Standard reconstruction resolution:
  - protons 2.6° - 1.4°
  - He, N better than p but worse than Fe
  - iron 2.3° - 1.2°
- DNN angular resolution:
  - protons: 2.5° - 1.0°
  - He, N better than p but worse than Fe
  - Iron slightly (<0.1°) better than protons

- Angular resolution **improves 0.2 °- 0.4°**

Core position resolution

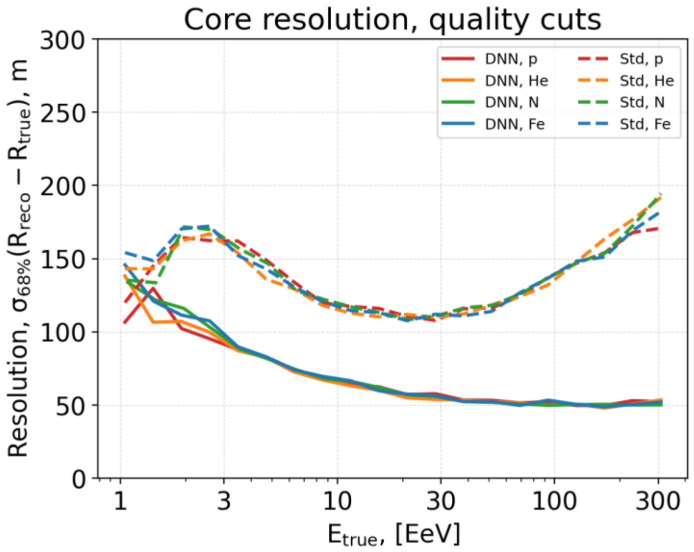

- Reconstruction after quality cut
- Standard reconstruction resolution:
  - 100 – 150 m
- DNN core resolution:
  - 50 – 80 m
- Similar for all elements

- Core resolution improves **1.5x** - **2x** using DNN
- DNN reconstruction equally good in parallel and perpendicular directions of shower axis projection

TA Hybrid data

Hybrid data:

- Detected both SD and FD
- 9 years: 2008-05-27 to 2017-11-28
- Total 3656 events,
- After quality cuts 911 events

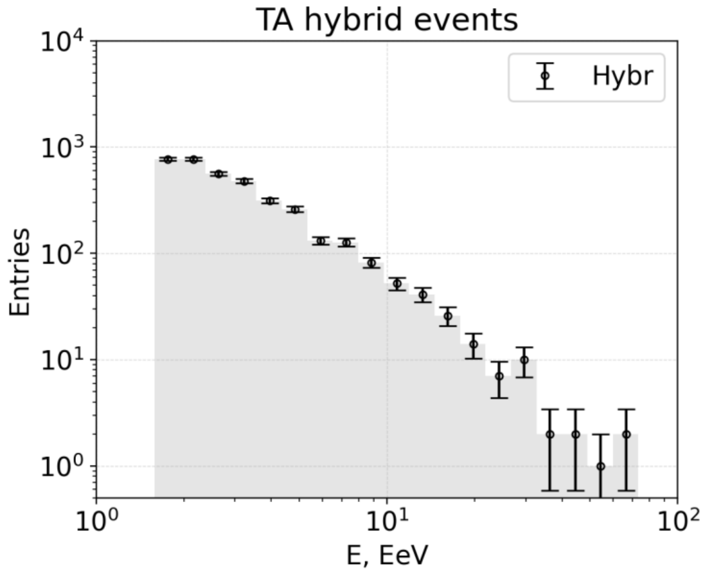

Performance on TA Hybrid data

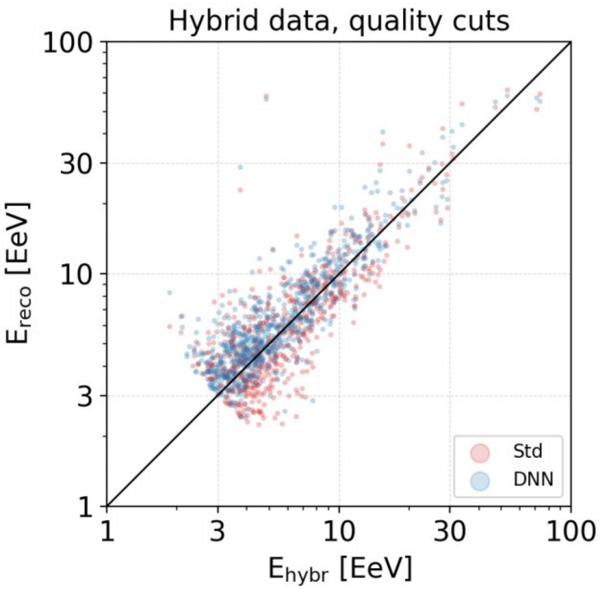

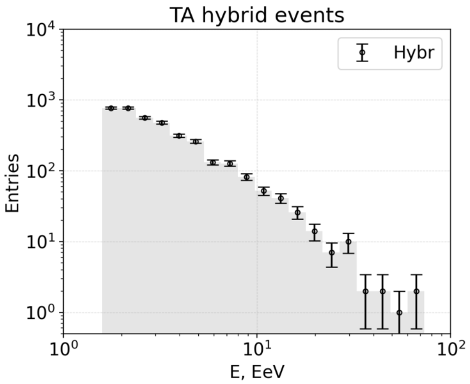

DNN works well on real TA data, with results similar to standard reconstruction

Hybrid data:

- Detected both SD and FD
- 9 years: 2008-05-27 to 2017-11-28
- Total 3656 events,
- After quality cuts 911 events

Calibration to FD

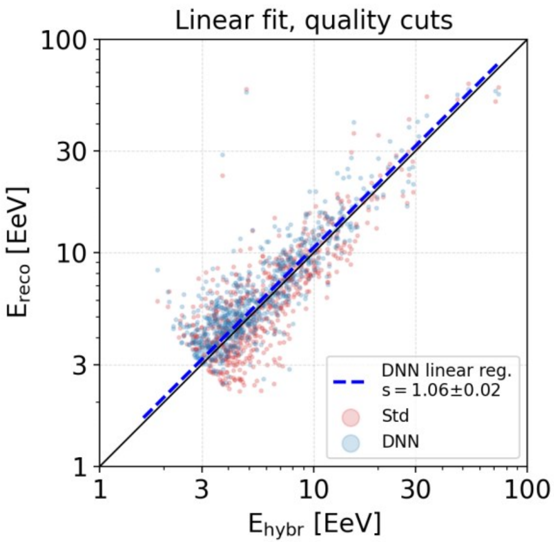

DNN * 1/1.06 ⇒
DNN calibrated to FD

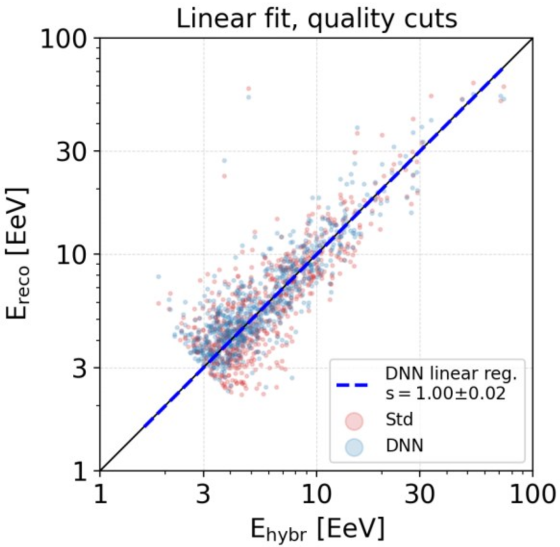

- Linear regression fit: E_{DNN} = s* E_{hybr}, bias = s - 1
- With offset 6% for DNN, the calibration factor for given DNN is s = 1.06
- In further application energy estimated with E = E_{DNN}/1.06

Conclusions

- We presented a new DNN reconstruction method for the Telescope Array Surface Detector.
- DNN improves the accuracy of Standard reconstruction for energy resolution, direction, and core position on events with quality cuts.
- Reasonable performance of DNN on events that haven’t passed quality cuts indicates that DNN could perform well on a larger dataset with more relaxed quality cuts.
- Validation on TA hybrid data shows that the DNN performs well on real data.
- Next steps include developing a new set of quality cuts and accuracy metrics for the DNN to effectively utilize available data while maintaining the accuracy of the reconstruction